PIP4Ks impact on PI3K, FOXP3 and UHRF1 signaling and modulate human regulatory T-cell proliferation and immunosuppressive activity.

Alessandro Poli [1,8*], Shidqiyyah Abdul-Hamid[2,9], Antonio Enrico Zaurito[3,8], Francesca Campagnoli[2,10], Valeria Bevilacqua[5], Bhavwanti Sheth[2], Roberta Fiume[4], Massimiliano Pagani[1,6], Sergio Abrignani[5,7] and Nullin Divecha[2,8*],

1. FIRC Institute of Molecular Oncology (IFOM), Via Adamello 16, Milan (IT)
2. Inositide Laboratory, School of Biological Sciences, Faculty of Environmental and Life Sciences, University of Southampton, Life Sciences Building 85, Highfield, Southampton SO17 1BJ, UK
3. Center for Translational Cancer Research (TranslaTUM), Klinikum rechts der Isar, Technische Universität München, Einsteinstraße 25, Munich (DE).
4. Department of Biomedical Sciences (DIBINEM), University of Bologna, Via Irnerio, 48, 40126 Bologna, Italy.
5. National Institute of Molecular Genetics (INGM) "Romeo ed Enrica Invernizzi", Via Francesco Sforza, 35, Milan (IT)
6. Department of Medical Biotechnology and Translational Medicine, University of Milan, Milan, Italy.
7. Department of Clinical Sciences and Community Health, University of Milan, Milan (IT)
8. Previous address: National Institute of Molecular Genetics (INGM) "Romeo ed Enrica Invernizzi", Via Francesco Sforza, 35, Milan (IT)
9. Department of Basic Medical Science, Faculty of Nursing, IIUM, Kuantan Pahang 25200, Malaysia
10. Department of Experimental Medicine (DIMES) L.go R. Benzi 10 Genova, 16131 Italy

* To whom correspondence should be addressed: alessandro. poli@ifom.eu and n.divecha@soton.ac.uk

Key words: T-cells, Tregulatory cells, lipid kinases, PIP4K, PI3K, UHRF1, FOXP3

Abstract

Regulatory T cells (Tregs) play fundamental roles in maintaining peripheral tolerance to prevent autoimmunity and limit legitimate immune responses, a feature hijacked in tumour micro-environments where recruitment of Tregs often extinguishes immune surveillance through suppression of T-effector cell signalling and tumour cell killing. Pharmacological tuning of Treg activity without impacting on T conventional (Tconv) cell activity would likely be beneficial in the treatment of various human pathologies. PIP4K2A, 2B and 2C constitute a family of lipid kinases that phosphorylate PtdIns5*P* to PtdIns(4,5)P_2. They are involved in stress signalling, act as synthetic lethal targets in p53 null tumours and in mice, loss of PIP4K2C leads to late onset hyperinflammation. Accordingly, a human SNP near the PIP4K2C gene is linked with susceptibility to autoimmune diseases. How PIP4Ks impact on human T cell signalling is not known. Using ex-vivo human primary T cells, we found that PIP4K activity is required for Treg cell signalling and immunosuppressive activity. Genetic and pharmacological inhibition of PIP4K in Tregs reduces signalling through the PI3K, mTORC1/pS6 and MAPK pathways, impairs cell proliferation and increases activation induced cell death, while sparing Tconv. PIP4K and PI3K signalling regulate the expression of the Treg master transcriptional activator FOXP3 and the epigenetic signalling protein Ubiquitin-like containing PHD and RING finger domains 1 (UHRF1). Our studies suggest that pharmacological inhibition of PIP4K can reprogram human Treg identity, while leaving Tconv cell signalling and Th differentiation largely intact potentially enhancing overall immunological activity.

Significance statement

PIP4Ks are druggable lipid kinases critical in cancer biology, whose function in human immunity remains unknown. Here we show that PIP4Ks specifically control growth and activity of a subset of human immune cells called Tregs, isolated from the blood of healthy donors. Tregs function to exquisitely control the strength of the immune response. If the immune response is too strong, this can trigger autoimmune disease insurgence, while weak responses can lead to increased infections or enable tumour cell growth. Being able to selectively control Treg activity would impact on the strength of immune responses and ultimately how we treat human diseases. Accordingly, we show that a drug like inhibitor of PIP4K can be used to control Treg cell activity.

Introduction

CD4+ T cells orchestrate the activation of the immune system, as well as suppressing uncontrolled immune reactions (1). CD4+ T cells with distinct effector or regulatory functions are characterized by well-defined cytokine profiles and transcriptional programs giving rise to T-helper (Th) cells, follicular T cells (Tfh) and regulatory T cells (Treg) (2, 3). Tregs are critical for the maintenance of immunological self-tolerance and negative control of immune responses to non-self antigens (4) and their loss leads to severe autoimmune diseases including type I diabetes, gastritis, and thyroiditis (4, 5). Circulating Tregs are generated in the thymus through positive selection of cells presenting high-affinity MHC class II restricted self-peptides (2, 3). Additionally peripheral Tregs can be generated through differentiation of CD4+ conventional T cells (Tconv) preferentially in peripheral lymphoid tissues (6, 7). Tregs express high levels of the Treg lineage specification transcription factor FOXP3 (Forkhead box P3) (5) (8-10) , which controls both their function and identity. Deletion of FOXP3 in Tregs leads to loss in suppressive activity (11), whilst, its heterologous overexpression confers suppressive activity to Tconvs (8-10). FOXP3 controls the expression of human Treg signature genes including IL2RA (which encodes CD25, IL-2 receptor alpha chain that enhances survival and IL-2 uptake), CTLA4, and TNFRSF18 (GITR) (12). In peripheral blood, Tregs represent approximately 1-5% of CD4+T cells, while in tumours they may represent up to 20-30% of the CD4+T cell repertoire (13). Tumour infiltration by Tregs is often associated with poor prognosis and Treg depletion can boost anti-tumour immune responses (13, 14). Thus, suppressing Treg function while maintaining Tconv activity could boost immune cancer cell killing and increase the capacity of immunotherapy in cancer treatment.

Polyphosphoinositides lipid messengers impact a wide array of cell processes including receptor-mediated control of cell proliferation and survival, migration and transcription. While studies have shown that genetic and pharmacological inhibition of the PI3K pathway in mice and in human patients reduces Treg suppressive activity (15, 16) (17), much less is known about the role of other PPIns pathways. The PIP4K family of lipid kinases phosphorylate PtdIns5*P* to generate PtdIns(4,5)P_2 (18). The three isoforms of PIP4Ks, 2A, 2B and 2C localise predominantly in the cytoplasm (19), the nucleus (19-22) and endomembranes (23) respectively and have redundant and non-redundant roles in vivo (19, 24, 25). PIP4K2A-/-_PIP4K2B+/- mice suppress tumour development in p53 null mice (24) and PIP4K2C knockout mice develop characteristics of hyper-inflammation (25). Moreover, a human SNP near the PIP4K2C gene associates with increased autoimmune diseases (26). These data suggest that PIP4K are intimately linked with immune responses.

Here we reveal that PIP4K2B and PIP4K2C are required for human Treg cell proliferation, survival and immuno-suppressive functions. Transcriptome and cell biological analyses revealed that PIP4K depletion reduces PI3K/AKT signalling and proliferation and increases activation induced cell death in Tregs, while leaving Tconv cell activation intact. Reduced Treg function was associated with reduced expression of the essential Treg epigenetic regulator Ubiquitin-like containing PHD and RING finger domains 1 (UHRF1)

and decreased expression levels of FOXP3. Moreover, pharmacological inhibition of PIP4K2C phenocopies its knockdown. These data identify the importance of PIP4K signalling in human Treg immunosuppressive function and illustrate that their inhibition can reprogram Treg cells while sparing Tconv cell signalling and Th cell differentiation.

Materials and Methods

Materials.

Antibodies and sh_RNA sequences are listed in SI Appendix, Table1, 2 and 4 and qRT-PCR probes in SI Appendix, Table3.

Isolation of Naive T cells, naive Treg and Tconv cells.

Naïve, Treg and Tconv cells were isolated from buffy coats of healthy donors obtained from Fondazione I. R. C. C. S. Ca'Granda Ospedale Maggiore Policlinico in Milan. Blood samples used in this study were de-identified before collection and manipulation. PBMC were purified on Ficoll-Paque PLUS (GE Healthcare) and CD4+ T cells were purified (CD4+ T cells isolation kit, Miltenyi). Subsequently, Naive (*CD4+, CD62l+, CD45RO-*), naive Treg (*CD4+, CD25+, CD127-, CD45RO-, CD62l+)* and Tconv cells (*CD4+, CD25-, CD127+, CD45RO-, CD62l+)* were isolated by FACS (BD FACS Aria).

Primary T cells stimulation, expansion and differentiation

Naive T cells were expanded using anti-CD3/CD28 (CD3/CD28) coated magnetic Dynabeads (Human T-Activator CD3/CD28, Life technology) for 5 days (Figure 1A). Freshly isolated naïve Treg cells were expanded using the rapid expansion protocol (REP) (27). For Treg differentiation, freshly sorted naive T cells were TCR stimulated for 5 days together with IL-2, TGFβ1 (5ng/ml, Sigma Aldrich). For Th1 or Th2 polarization, naive T cells were TCR stimulated and cultured with IL-2, IL-12 (10ng/ml, Miltenyi), anti-IL-4 (2μg/ml, Miltenyi) or with IL-2, IL-4 (10ng/ml, Miltenyi), anti-IFNγ (2 μg/ml, Miltenyi) and anti-IL12 (2 μg/ml, Miltenyi) respectively for 8 days.

Immunostaining

PBMC were washed with PBS and cell surface antigens were stained at 37°C using specific conjugated antibodies. For intracellular staining, cells were fixed, permeabilised using Fixation/Permeabilization Buffer (eBioscience) at 4'C and then incubated with specific conjugated antibodies (Supplementary Table A) diluted in Permeabilization Buffer (Life Technologies). After washing cells were analysed using FACS (Canto II (BD)).

Molecular Cloning

pLKO_1 vectors targeting specific genes were purchased from Sigma Aldrich (sh_Mission). Puromycin resistance sequence was substituted with sequences encoding either GFP or mCherry. pCDH vectors were purchased from System Bioscience, and PIP4K2B or PIP4K2C coding sequences were inserted between XbaI/BamHI restriction sites. All plasmids are available upon request.

Lentiviral production and primary T cells transduction

Lentiviral particles were produced in Hek293T cells, mixed with Polybrene (8μg/ml) and used to transduce $5x10^5$ TCR stimulated Naive T, Tconv or Treg cells by spinoculation for 20 minutes at 2000 rpm. Cells were seeded in RPMI1640 10% FBS supplemented with IL-2 or treated as above to induce differentiation into Treg or Th1/Th2 cells. GFP/mCherry positive cells were FACS sorted and analysed.

PIP4K, PI3K, mTORC1 inhibition

Naïve T, Treg and Tconv cells were treated with NIH-12848 (10:30μm), CAL-101 (10μm) and Rapamycin (100nm) to inhibit PIP4K2C, PI3Kδ and mTORC1 signalling respectively. Treg differentiation studies used Naïve T cells freshly isolated from peripheral blood treated with inhibitors as above and differentiated into Treg cells as described. For analysis of UHRF1 or FOXP3 levels, Tregs expanded by REP were treated with NIH-12848 or CAL-101 for 24 or 48 hours and analysed by RT-qPCR or FACS. shRNA silenced cells were treated with inhibitors and TCR re-stimulated for 48h. Finally, for analysis of cell viability, cell proliferation and suppressive capacity of Tregs, cells were treated with the indicated doses of NIH-12848 for 48h. DMSO was used as vehicle control in the experiments.

Tconv cell suppression Assay

Naive T cells were labelled with Cell Trace (Violet or CFSE, Thermo Fischer) and co-cultured with or without Treg cells at specified target to effector ratios. Cells were stimulated with CD3/CD28 (1 cell : 0. 1 bead) without IL-2 for 4 days (28). Proliferation was quantitated by dilution of Cell Trace/ FSE using FACS and analysed using Flow. Jo 8/10.

Interleukin production assay

Interleukin production was assessed in the presence of brefeldin-A after stimulation with PMA (50 ng/ml) and Ionomycin (1μM) (29) using FACS.

Proliferation Assay

Cell Trace (Violet/CSFE, Thermo Fischer) labeled primary Treg or Tconv cells were stimulated with CD3/CD28 (1 cell : 0. 1 bead) for 4 days. Proliferation was monitored by dilution of Cell Trace / CFSE using FACS.

Cell Cycle Analysis

Cells were stimulated for 3 days, washed in PBS and fixed in cold EtOH 70% overnight. Cells were washed with PBS and stained with Propidium Iodide (Abcam) and analysed by FACS.

Cell Viability Analysis

Cells were resuspended in Annexin V resuspension buffer and stained with Annexin V-APC (BioLegend) for 20 minutes at room temperature and then directly analysed by FACS. Live/Dead cell staining (ThermoFischer) was used following manufacturer's instructions.

qRT-PCR

Cells were lysed and RNA was extracted using a silica column (see supplementary methods). cDNA was synthesised using a Reverse-transcription Kit (Life Technologies). qRT-PCR was performed using SYBR Green (Life Technologies). qRT-PCR was performed using SYBR Green (Life Technologies), and gene expression changes were normalised to GAPDH as housekeeping control.

Western Blotting

Cell lysates were separated on bis-tris discontinuous SDS page gels, electroblotted to nitrocellulose, blocked in PBS-Tween-20 (0. 1%)-dried milk (5%) and then incubated with the primary antibodies diluted appropriately in PBS-Tween-20 (0. 1%) containing 1:50 dilution of Roche blocking buffer. After washing

blots were incubated with appropriate secondary antibodies conjugated to HRP or fluorescent dyes and visualised by chemiluminescence or Licor imaging respectively. For analysis of signalling pathways, Treg and Tconv cells isolated and expanded through REP were transduced to silence PIP4K or treated with inhibitors (48h), re-stimulated with anti-CD3/CD28 dynabeads for 1h. List of Ab used in this work is reported in Table 4.

RNA sequencing

RNA was extracted and sequenced by Novogene (Paired end 150 bp). The reads were clipped to a max score and to a length of 120bp using Trimmomatic and aligned to the human reference genome (GRCh38) using HISAT2. Gene level quantitation and differential expression was determined using FeatureCounts and DESeq2. An excel file is provided which contains a summary of the donors and shRNA (DatasetS1 A), expression data (Dataset, statistics for GSEA analysis, comparison tables for and the normalized count data (DatasetS1). Principal component analysis (PCA) and gene ontology analysis was carried out using prcomp and ClusterProfiler respectively and heatmaps were generated in Pheatmap. Volcano plots were generated using R package DeBrowser.

Statistical Analysis

In all figures n refers to cells isolated from different donors. Statistical analysis was performed employing two-way unpaired t-test or paired t-test using Prism 9. *pVal<0.05, **pVal<0.01, ***pVal<0.001 unless otherwise stated.

Results

PIP4K2B or 2C depletion impairs FOXP3 up-regulation and Treg differentiation of stimulated CD4+ T cells while sparing Th specific transcription factors.

Antigen-MHC activation of Naive CD4+ T cells in the presence of specific cytokines induces their differentiation into distinct populations of T cells controlling immune responses to diverse organisms and foreign bodies (1). IFN-γ and IL-12 drive Th1 differentiation, which express the lineage specification factor T-Bet (T-box transcription factor TBX21) (30). Th2 differentiation is mainly driven by IL-4 which upregulates the transcription factor GATA3 (GATA binding protein) while IL6, IL21, IL23, and TGF-β drive Th17 differentiation and the expression of RORγτ (retinoic acid receptor-related orphan receptor gamma-T) transcription factor (31, 32). Although Tregs mainly differentiate in the thymus after antigen priming, TGF-β can induce peripheral Treg cell commitment by triggering FOXP3 expression in naïve T cells (33). Since *in vitro* TCR-mediated stimulation of Naïve T-cells induces transient expression of these master transcription factors (34, 35), we analysed if PIP4K depletion (sh_2B/sh_2C) impacted on their expression. Naive CD4+ T cells were sorted by FACS, stimulated with anti-CD3/CD28 coated beads, transduced with lentiviruses to silence different PIP4K isoforms and GFP/mCherry positive cells were selected by FACS. Up to 90% of Tconv cells were positively transduced (Figure 1A) and qRT-PCR (Figure 1B) revealed sh-mediated isoform selective knockdown of PIP4K gene expression by 60-85% compared to control samples (sh_Ctrl).

Surprisingly, knockdown of PIP4K2B or PIP4K2C impaired FOXP3 mRNA and protein accumulation (Figure 1C and 1D) but not T-bet or GATA3 (Figure 1C and 1D) and slightly increased RORγ–τ expression (SI Appendix, Supp_Figure_1A). Depletion of PIP4K2B or 2C in Tconv cells did not strongly affect lineage specific cytokines synthesis such as IL-4 (Th2) or IFNγ (Th1) (SI Appendix, Supp_Figure_1B and 1C), confirming a lack of impact on Th polarisation.

As PIP4K signalling impacts on FOXP3 expression in Naïve T cells, we tested how their depletion might regulate *in vitro* induction of Treg cells. Differentiation of Naïve T cells towards Tregs can be induced *in vitro* through TCR stimulation in the presence of TGFβ1 and IL-2 (33), leading to strong up-regulation of FOXP3 expression (Figure 1F). Strikingly, accumulation of both FOXP3 mRNA (Figure 1E) and protein (Figure 1F and 1G) were impaired by depletion of PIP4K2B or 2C. A reduction in the accumulation of FOXP3 mRNA and protein was observed using 4 different sh_RNA targeting constructs per isoform (SI Appendix Supp_Figure_1D, 1E and 1F). Depletion of PIP4K2A had no effect on FOXP3 accumulation (SI Appendix, Supp_Figure_1G). On the contrary, Th1 (driven by T-bet) and Th2 (driven by GATA3) differentiation was not changed by PIP4K2B or 2C depletion (SI Appendix, Supp_Figure_2A, B, C, D), and did not alter IFNγ synthesis in Th1 cells (SI Appendix, Supp_Figure_2E) but did slightly reduce IL-4 synthesis in Th2 cells (SI Appendix, Supp_Figure_2F). These data suggest that depletion of PIP4Ks leave Th1 or Th2 differentiation pathways intact but impair *in vitro* Treg induction. To better define how

PIP4K2B and 2C impact on FOXP3 expression and Treg function, we investigated their impact on CD4+FOXP3+Tregs isolated from peripheral blood of healthy donors.

PIP4K2B and PIP4K2C are required for Treg cell mediated immunosuppression.

Circulatory Tregs can be subdivided in different subsets (3) depending on the expression of FOXP3 and CD45RA markers (7). Naïve Tregs (herein referred to as Tregs) isolated by FACS (CD4+/CD25^{high}/CD127-/CD45RO-) showed high FOXP3 expression compared to conventional T cells (CD4+/CD25^{low}/CD127+/CD45RO-) (Figure 2A and 2B). Depletion of PIP4K2B or 2C in expanded Tregs using 4 different sh_RNAs per isoform (Figure 2C) impaired FOXP3 protein expression (Figure 2D and 2E) reduced TCR activated FOXP3 induction (SI Appendix Supp_Figure_3A and 3B). PIP4K2A depletion did not change FOXP3 protein levels (SI Appendix, Supp_Figure_3C). 2B). Conversely, PIP4K2B or 2C overexpression slightly increased FOXP3 expression in stimulated naïve T cells and *in vitro* differentiated Treg cells (SI Appendix, Supp_Figure_3D and 3E) and in Treg cells (SI Appendix, Supp_Figure_3F, 3G and 3H). Moreover, exogenous overexpression of PIP4K2B or 2C rescued decreased FOXP3 levels in Treg cells after depletion of endogenous PIP4Ks (Figure 2D and 2E, SI Appendix, Supp_Figure_3G and 3H). Interestingly, combined depletion of PIP4K2B and 2C (SI Appendix, Supp_Figure_3I) more strongly decreased FOXP3 expression compared to depletion of either PIP4K alone (SI Appendix, Supp_Figure_3J). Continuous FOXP3 expression maintains Treg immunosuppressive activity (36) and therefore, we assessed if PIP4K depletion in Tregs impacts on their immuno-suppressive function. CD3/CD28 stimulated strong proliferation in Tconv cells, which was dose dependently inhibited by control Tregs. However, knockdown of either PIP4K2B or 2C in Tregs reduced their capacity to suppress Tconv cell proliferation. Strikingly, combined knockdown of PIP4K2B and 2C more strongly attenuated Treg suppressive activity (Figure 2F and 2G and SI Appendix, Supp_Figure_4A and 4B). In contrast, PIP4K2B or 2C overexpression in Tregs increased Treg immunosuppressive activity (SI Appendix, Supp_Figure_4C). Tregs express many proteins involved in suppressive activity and also upregulate the expression of particular proteins within specific physiological and tumour induced microenvironments (37, 38). We assessed the expression of some of these in response to PIP4K depletion but found only the expression of CTLA4, a FOXP3 target, was decreased by PIP4K2B/2C depletion (SI Appendix, Supp_Figure_5A). CTLA4 is critical for Treg suppressive function (39) and FOXP3 knockdown reduced CTLA4 expression (SI Appendix, Supp_Figure_5B). These data show that PIP4K2B and 2C impact on FOXP3 and CTLA4 expression to control Treg immunosuppressive activity.

Depletion of PIP4Ks reprogram the Treg transcriptome.

PIP4K2B or 2C were depleted using two different sh_RNA in Treg and Tconvs isolated from two different donors (SI Appendix Supplementary Materials). PIP4Ks were not differentially expressed in Tconv

compared to Tregs (SI Appendix, Supp_Figure_6A) and PIP4K depletion reduced FOXP3 expression in Tregs (SI Appendix, Supp_Figure_6B). The transcriptome of these cells was analysed using RNA-seq. After mapping reads to the genome, quantitation at the gene level was assessed and differentially expressed genes extracted using DESeq2. Volcano plots show PIP4K2B depletion changed the expression of 2569 genes (FDR<0. 05 and absolute log2 fold change (LFC) >0. 6) while PIP4K2C depletion changed 524 genes (FDR<0. 05 and absolute LFC >0. 6) (Figure 3A). The volcano plots also highlight how more genes were significantly changed in Tregs compared to Tconv cells after depleting PIP4K (DatasetS1 E-H). The differentiation and function of Tconvs was largely unchanged after depleting PIP4K and accordingly knockdown of PIP4K2B or 2C in Tconv cells changed only 135 and 66 genes respectively (FDR=0. 05 and absolute LFC >0. 6, DatasetS1 B, Figure 3B). As depletion of either PIP4K2B or 2C decreased FOXP3 expression and inhibited Treg suppressive activity we searched for genes that were coregulated in both knockdowns. There was a highly significant degree of overlap of genes regulated in Tregs by both PIP4K2B and PIP4K2C (230 genes: representation factor 3.4 and $p<2.34x10^{-71}$) (SI Appendix, Supp_Figure_6C-VennDiagram). Given this, we reanalysed the RNA-seq data combining both sh_2B and sh_2C depleted Treg samples to generate a PIP4K2B_2C regulated geneset (Treg_shPIP4K-DEG: 219 genes up and 200 genes down: *p*-adjusted<0.05 and absolute LFC >0. 6). Deregulation of Treg_shPIP4K-DEG by depletion of either PIP4K2B (Treg:log(sh_2B/sh_Ctrl) or 2C (Treg:log(sh_2C/sh_Ctrl) in Tregs was highly correlated (Figure 3C, R=0.93). However, this geneset was only weakly deregulated by PIP4K2B or 2C depletion in Tconv cells (Figure 3C). Strikingly, genes differentially expressed in Tconv after knock down of PIP4K were not changed in Tregs (SI Appendix, Supp_Figure_6D). PCA analysis using Treg_shPIP4K-DEG genes show that PC1 and PC2, which account for 90% of the variation, strongly distinguish control and PIP4K depleted Tregs as expected (Figure 3D). Surprisingly, Treg_shPIP4K-DEG also strongly distinguish Tconv cells from Tregs. Moreover, the PCA analysis confirmed the lack of a strong effect of PIP4K depletion in Tconv as all Tconv samples clustered closely together regardless of PIP4K depletion. To further explain the PCA analysis we generated heatmaps to visualise the expression of Treg_shPIP4K-DEG in different T cell groups. The expression profile of Treg_shPIP4K-DEG was clustered into three groups Cluster 1, Cluster 2 and Cluster 3 (Figure 3E left panel) and the average expression of genes within each cluster was quantitated (Figure 3E right panel). Cluster 1 genes were significantly upregulated in Tregs after depletion of either PIP4K2B or 2C and were more highly expressed in Tconv compared to Treg regardless of whether PIP4K were depleted. Cluster 2 genes were significantly downregulated in Tregs after depletion of PIP4K and had decreased expression in Tconv compared to Treg. In Tconv, Cluster 2 gene expression was not further changed by depletion of PIP4K. Cluster 3 genes were decreased in Tregs after knockdown of either PIP4K2B or 2C but their expression in Tconv was similar to control Tregs and did not show any change upon knockdown of PIP4K. The altered expression of some of the deregulated genes was verified using qRT-PCR of RNA extracted from both Treg and Tconv cells from different patient donors using qRT-PCR (SI Appendix, Supp_Figure Figure 6E). For example, the

expression of HMOX1 and BAIAP3 is strongly upregulated by either PIP4K2B or 2C depletion in Tregs and slightly upregulated in Tconv cells (cluster1). PLK1 and FOXP3 are down regulated mainly in Tregs (cluster 2). PKMYT1, TK1 and IQGAP3 and UHRF1 (see later) are down regulated in Tregs, while their expression in Tconv mirrors their expression in Treg control cells (cluster 3). Similar downregulation of Treg_shPIP4K-DEG was observed in an unrelated dataset comprising Tregs and Tconv isolated from 12 different healthy donors (GSE166866. SI Appendix, Supp_Figure Figure 6F). These data suggest that depletion of PIP4Ks in Tregs reprograms the expression of many genes to mirror their expression in Tconv cells (cluster 1 and 2). The differential effects on gene expression observed on depletion of PIP4K supports our contention of different functional roles for PIP4Ks in Tregs compared to Tconvs. Cluster 3 genes are particularly intriguing as they are decreased in Tregs upon depletion of PIP4K but are expressed to the same extent as control Tregs. We isolated cluster 3 genes and used them to interrogate an unrelated RNA-seq data set comprising human Tconv and Tregs before and after T cell stimulation (CD3/CD28) isolated from four patient donors (GEO GSE138603). Cluster 3 genes were more highly expressed in Tconv compared to Tregs in the basal state. Surprisingly, cluster 3 genes are strongly upregulated in response to T cell activation (Figure 3F) in both Tconv and Tregs. Gene ontology analysis showed that Cluster 3 genes were highly enriched for genes involved in cell cycle, chromosome segregation and mitosis (Figure 3G). Cluster 1 and 2 genes were enriched for autophagy and translation terms respectively (SI Appendix, Supp_Figure 6G and H). These data suggest that PIP4K depletion specifically decreases the expression of a subset of T cell activation dependent genes in Tregs without impacting on their expression in Tconv.

PIP4K specifically control PI3K/mTORC1 pathways in activated Treg cells.

Since RNAseq analysis indicated that the expression of a subset of T-cell activation dependent genes involved in cell cycle and mitosis were deregulated in Tregs but not in Tconv (cluster 3), we investigated if and how PIP4Ks might differentially control specific signalling pathways stimulated by T cell activation. PIP4K2B and 2C impact on PI3K, mTORC1 signalling (24, 25, 40) and MAPK signalling (21, 24). Stimulation with CD3/CD28 activated the PI3K/mTOR and MAPK pathways in both Tregs and in Tconv with similar time courses (SI Appendix, Supp_Figure_7A and 7B). PIP4K2B or 2C depletion in Tregs strongly attenuated CD3/CD28 activation of Akt, pS6 and ERK (Figure 4A and quantitated in 4B top panels), while their depletion in Tconv had little impact (Figure 4A and quantitated in 4B lower panels). PI3K and mTORC1 signalling positively contribute to activated T cell viability and proliferation (41) but have different roles in T cells (17, 42, 43). We next analysed how PIP4K2B or 2C depletion impacts on proliferative capacity and cell viability of Tregs and Tconvs. Tregs exhibited decreased proliferation when PIP4K2B or 2C was depleted (Figure 4C and Figure 4D top panels) which was not observed in Tconv cells (Figure 4C and Figure 4D lower panels) and was characterised by decreased cell numbers in S and G2/M phases of the cell cycle (SI Appendix, Supp_Figure_7C) and decreased Ki67 staining (SI Appendix, Supp_Figure_7D). Moreover, PIP4K2B or 2C depletion stimulated TCR activation-induced cell death in

Tregs (Figure 4E and Figure 4F top panels) but not in Tconvs (Figure 4E and Figure 4F lower panels). Silencing of PIP4K2A had no effects on Treg cell proliferation or viability (SI Appendix, Supp_Figure_7E, 7F, and 7G). These data confirm a stronger role for PIP4K2B and 2C in controlling signalling, proliferation and viability in Tregs compared to Tconvs.

PI3K inhibition decreases FOXP3 levels in in Tregs.

Since PI3K and mTORC1 signalling were altered by PIP4K, we investigated the relationship between activation of these pathways and FOXP3 expression, by their direct inhibition. Rapamycin treatment attenuated phosphorylation of S6, a downstream target of mTORC1, but not phosphorylation of AKT. Treatment with CAL-101 (PI3Kδ inhibitor) attenuated phosphorylation of both AKT and pS6 (SI Appendix, Supp_Figure_7H). Treatment of Tregs with CAL-101 but not Rapamycin decreased expression of FOXP3 in Treg cells (Figure 4G) and decreased FOXP3 accumulation in *in vitro* differentiated Treg (Figure 4H). CAL-101 also decreased FOXP3 expression after CD3/CD28 stimulation (SI Appendix, Supp_Figure_7I). Interestingly, combined PI3Kδ inhibition with depletion of either PIP4K2B or 2C almost completely attenuated the CD3/CD28 mediated increase in FOXP3 levels (SI Appendix, Supp_Figure_7I). These data suggest that PIP4K utilises PI3K dependent and independent pathways to impact on FOXP3 expression.

PIP4K, PI3K and UHRF1 signalling controls FOXP3 expression and Treg function.

To further delineate how PIP4K signalling impacts on FOXP3 expression and Treg proliferation while sparing Tconv cells, we investigated genes from cluster 3. UHRF1 encodes a nuclear E3-ubiquitin ligase that interacts with and recruits DNA methyltransferases to control DNA methylation (44). UHRF1 is a key regulator of Treg differentiation, maintenance and activity (45, 46), and is allosterically regulated by PtdIns5P, the substrate for PIP4K (47). Furthermore, the levels of UHRF1 and FOXP3 mRNA changed co-ordinately after CD3/CD28 stimulation (Figure 5A), demonstrating that their expressions are both T cell activation dependent. We confirmed that depletion of PIP4K2B or 2C decreased UHRF1 mRNA levels in human Treg cells but not in Tconv cells (Figure 5B) and decreased UHRF1 protein expression (Figure 5C). Treatment of Tregs with the PI3Kδ inhibitor, CAL-101, strongly inhibited UHRF1 expression and subsequently impaired FOXP3 expression (Figure 5D). These data suggest that UHRF1 couples PIP4K/PI3K signalling to FOXP3 gene regulation. To directly implicate UHRF1 in the control of FOXP3 expression we showed that depletion of UHRF1 using two different sh_RNAs decreased FOXP3 mRNA (Figure 5E) and protein levels (Figure 5F and 5G) and reduced CTLA4 protein expression (Figure 5H and 5I). Importantly, UHRF1 depletion reduced Treg suppression of Tconv cell proliferation (Figure 5J), and increased apoptosis in Tregs (Figure 5K). These data indicate that UHRF1 silencing phenocopies PIP4K depletion in Tregs, and that depletion of UHRF1 or PIP4K leads to two differentially regulated phenotypes. The first is decreased expression of FOXP3 and immunosuppression. The second is an increase in cell death and a decrease in cell proliferation. That these phenotypes are not related is illustrated by a lack of cell cycle

blockade or increased apoptosis in Tregs after knockdown of FOXP3, although there is a decrease in CTLA4 levels (SI Appendix, Supp_Figure_8A and 8B). Analysis of FOXP3 expression in live or dead cells isolated by FACS clearly demonstrated that reduced FOXP3 expression is not a consequence of PIP4K depletion induced cell death (SI Appendix, Supp_Figure_8C). These data are consistent with a pathway in which PIP4K2B and 2C impact on PI3K and UHRF1 signalling to control FOXP3 expression and Treg immunosuppressive activity. Additionally, PIP4K and UHRF1 signalling control Treg cell proliferation and apoptosis independently of FOXP3.

Pharmacological inihibition of PIP4K2C phenocopies gene knockdown.

Given the recent interest in PIP4K inhibitors and to test if PIP4K activity underlies suppression of Treg function, we next tested if an irreversible inhibitor targeting PIP4K2C, NIH-12848 (48) might phenocopy PIP4K2C depletion in human Treg cells. NIH-12848 attenuated CD3/CD28 mediated stimulation of phosphorylation of AKT, pS6 and MAP kinase in Tregs (Figure 6A) but had little effect on the same pathways in Tconv (SI Appendix, Supp_Figure_9A). NIH-12848 dose dependently inhibited CD3/CD28 stimulated proliferation (Figure 6B), increased apoptosis (Figure 6C), impaired FOXP3 expression in Tregs (Figure 6D) and suppressed induction of *in vitro* Treg differentiation from Naive T cells (SI Appendix, Supp_Figure_9B). Importantly, NIH-12848 impaired Treg suppressive activity on Tconv proliferation (Figure 6E and SI Appendix, Supp_Figure_9C).

Our studies illustrate that pharmacological inhibition or depletion of PIP4K can be used to suppress Treg cell proliferation, survival and immunosuppressive activity while largely sparing Tconv cell signalling and Th differentiation (SI Appendix, Supp_Figure_10).

Discussion

We show that genetic and pharmacological inhibition of two isoforms of PIP4K lipid kinases regulate FOXP3 dependent and independent pathways to suppress human Treg function in three ways. Firstly, they control signalling through the PI3K, mTORC1/pS6 and MAPK pathways. Secondly, they impact on Treg proliferation and apoptosis. Thirdly, they control the expression of the master transcriptional regulator FOXP3 and more broadly reprogram Treg cell transcription profiles. Importantly, PIP4K2B or 2C depletion in Tconvs does not attenuate PI3K and mTORC1 signalling, Th differentiation and has little impact on transcriptional output. Moreover, PIP4K affect the expression of a subset of T-cell dependent activation genes involved in cell cycle control only in Tregs. PIP4K silencing does reduce FOXP3 expression in activated Tconvs and reduces their differentiation into Treg *in vitro*. Broadly, PIP4K depletion, would be expected to engender a hyperinflammatory environment *in vivo*, which is observed in PIP4K2C knockout mice (25) and implicate deregulation of Treg cells in the enhanced tumour suppression observed in PIP4K knockout mice (24). Interestingly, the non-redundancy of PIPK2B and 2C in human Treg immunosuppression suggests that Treg activity could be rheostatically controlled by using inhibitors that target one or both of the PIP4K isoforms in combination with clinically relevant inhibitors of PI3Kδ.

PIP4Ks control PtdIns5*P* and PtdIns(4,5)P_2 levels in a kinase dependent (21, 40) and independent manner (49). PIP4Ks impact positively and negatively on PI3K/Akt signalling (40, 49-51) but in Tregs we show that PIP4K2B and 2C depletion inhibits PI3K/mTOR. The decrease in T-cell activation signalling imparted by PIP4K silencing in Tregs is reflected by decreased expression of a subset of activation dependent genes involved in cell cycle, mitosis and chromosome segregation. These changes might explain the specific effect of PIP4K depletion on Treg proliferation and apoptosis compared to Tconv. Treg specific inhibition has also been observed with PI3Kδ inhibitors (16, 17)

PIP4K2B is localized to the cytosol and nucleus (22), suggesting it may directly regulate gene transcriptional output. PIP4K2B controls nuclear PtdIns5*P* which binds to nuclear proteins to modulate epigenetic signalling and transcriptional output (20, 52). Moreover, nuclear PtdIns5*P* allosterically regulates UHRF1 (47) directly linking PIP4K to the regulation of DNA methylation. UHRF1 appears to be a common mediator of PIP4K/PI3K dependent changes in immunosuppression and proliferation (SI Appendix, Supp_Figure_10). In mice UHRF1 limits Treg and Tconv to Treg differentiation (53) (54), while UHRF1 (45) (55) and its partner, DNA methylase DNMT1, (56) are essential in Tregs for cell proliferation, FOXP3 and CTLA4 expression and immunosuppressive activity. In mice UHRF1 depletion in Tregs is associated with increased incidences of inflammatory diseases and enhanced tumour immunity (45, 55). Interestingly, reducing UHRF1 levels in tumor cells leads to the re-expression of tumour suppressor genes and a reduction of tumor cell growth (57). These data suggest that the anti-tumour effects of PI3K and PIP4K inhibition observed *in vivo*, might in part be executed through deregulation of UHRF1 expression in Tregs and perhaps more broadly in tumor cells.

The discovery that cell autonomous inhibition of PIP4Ks can inhibit tumor cell growth (24) (58, 59) has stimulated the development of PIP4K inhibitors (48, 60). Roles for PIP4K in reprogramming human Treg cells to attenuate their immunosuppressive activity, while sparing Tconv cell signalling and Th differentiation and thereby potentially enhancing tumour immunosurveillance increases the relevance of these PIP4K inhibitors as anti-cancer therapeutics.

Acknowledgments. We acknowledge Marie Curie fellowship (nuc-inositide: ID 625639 2015-2017.) INGM, the Malaysian government and the BBSRC for funding (BB/P003508/1). We thank Dr. Mariacristina Crosti, Dr. Tiziano Donnarumma Prof. Klaus Okkenhaug and Dr. Jonathan H. Clarke for help and reagents and Dr. Paolo Maiuri for scientific support

Author contributions. SAH,FC,BS,AEZ,VB and RF contributed to aquisition and analysis of the data. MP and SA contributed to the design of the study. AP and ND contributed to the conception, design, aquisition,analysis and interpretation of the data. AP and ND wrote the paper. All authors have approved the submitted paper.

Conflict-of-interest disclosure: The authors declare no competing financial interests.

References.

1. R. V. Luckheeram, R. Zhou, A. D. Verma, B. Xia, CD4(+)T cells: differentiation and functions. *Clin Dev Immunol* 2012, 925135 (2012).
2. S. Z. Josefowicz, L. F. Lu, A. Y. Rudensky, Regulatory T cells: mechanisms of differentiation and function. *Annu Rev Immunol* 30, 531-564 (2012).
3. M. O. Li, A. Y. Rudensky, T cell receptor signalling in the control of regulatory T cell differentiation and function. *Nat Rev Immunol* 16, 220-233 (2016).
4. S. Sakaguchi, T. Yamaguchi, T. Nomura, M. Ono, Regulatory T cells and immune tolerance. *Cell* 133, 775-787 (2008).
5. D. A. Vignali, L. W. Collison, C. J. Workman, How regulatory T cells work. *Nat Rev Immunol* 8, 523-532 (2008).
6. R. A. Gottschalk, E. Corse, J. P. Allison, TCR ligand density and affinity determine peripheral induction of Foxp3 in vivo. *J Exp Med* 207, 1701-1711 (2010).
7. M. Miyara *et al.*, Functional delineation and differentiation dynamics of human CD4+ T cells expressing the FoxP3 transcription factor. *Immunity* 30, 899-911 (2009).
8. M. R. Walker *et al.*, Induction of FoxP3 and acquisition of T regulatory activity by stimulated human CD4+CD25- T cells. *J Clin Invest* 112, 1437-1443 (2003).
9. S. Hori, T. Nomura, S. Sakaguchi, Control of regulatory T cell development by the transcription factor Foxp3. *Science* 299, 1057-1061 (2003).
10. J. D. Fontenot, M. A. Gavin, A. Y. Rudensky, Foxp3 programs the development and function of CD4+CD25+ regulatory T cells. *Nat Immunol* 4, 330-336 (2003).
11. R. S. Wildin *et al.*, X-linked neonatal diabetes mellitus, enteropathy and endocrinopathy syndrome is the human equivalent of mouse scurfy. *Nat Genet* 27, 18-20 (2001).
12. C. Chen, E. A. Rowell, R. M. Thomas, W. W. Hancock, A. D. Wells, Transcriptional regulation by Foxp3 is associated with direct promoter occupancy and modulation of histone acetylation. *J Biol Chem* 281, 36828-36834 (2006).
13. A. Tanaka, S. Sakaguchi, Regulatory T cells in cancer immunotherapy. *Cell Res* 27, 109-118 (2017).

14. T. J. Curiel *et al.*, Specific recruitment of regulatory T cells in ovarian carcinoma fosters immune privilege and predicts reduced survival. *Nat Med* 10, 942-949 (2004).
15. D. T. Patton *et al.*, Cutting edge: the phosphoinositide 3-kinase p110 delta is critical for the function of CD4+CD25+Foxp3+ regulatory T cells. *J Immunol* 177, 6598-6602 (2006).
16. K. Ali *et al.*, Inactivation of PI(3)K p110delta breaks regulatory T-cell-mediated immune tolerance to cancer. *Nature* 510, 407-411 (2014).
17. S. Chellappa *et al.*, The PI3K p110delta Isoform Inhibitor Idelalisib Preferentially Inhibits Human Regulatory T Cell Function. *J Immunol* 202, 1397-1405 (2019).
18. L. E. Rameh, K. F. Tolias, B. C. Duckworth, L. C. Cantley, A new pathway for synthesis of phosphatidylinositol-4,5-bisphosphate. *Nature* 390, 192-196 (1997).
19. Y. Bultsma, W. J. Keune, N. Divecha, PIP4Kbeta interacts with and modulates nuclear localization of the high-activity PtdIns5P-4-kinase isoform PIP4Kalpha. *Biochem J* 430, 223-235 (2010).
20. O. Gozani *et al.*, The PHD finger of the chromatin-associated protein ING2 functions as a nuclear phosphoinositide receptor. *Cell* 114, 99-111 (2003).
21. D. R. Jones *et al.*, Nuclear PtdIns5P as a transducer of stress signaling: an in vivo role for PIP4Kbeta. *Mol Cell* 23, 685-695 (2006).
22. A. Ciruela, K. A. Hinchliffe, N. Divecha, R. F. Irvine, Nuclear targeting of the beta isoform of type II phosphatidylinositol phosphate kinase (phosphatidylinositol 5-phosphate 4-kinase) by its alpha-helix 7. *Biochem J* 346 Pt 3, 587-591 (2000).
23. J. H. Clarke, P. C. Emson, R. F. Irvine, Localization of phosphatidylinositol phosphate kinase IIgamma in kidney to a membrane trafficking compartment within specialized cells of the nephron. *Am J Physiol Renal Physiol* 295, F1422-1430 (2008).
24. B. M. Emerling *et al.*, Depletion of a putatively druggable class of phosphatidylinositol kinases inhibits growth of p53-null tumors. *Cell* 155, 844-857 (2013).
25. H. Shim *et al.*, Deletion of the gene Pip4k2c, a novel phosphatidylinositol kinase, results in hyperactivation of the immune system. *Proc Natl Acad Sci U S A* 113, 7596-7601 (2016).
26. S. Raychaudhuri *et al.*, Common variants at CD40 and other loci confer risk of rheumatoid arthritis. *Nat Genet* 40, 1216-1223 (2008).
27. M. E. Dudley, J. R. Wunderlich, T. E. Shelton, J. Even, S. A. Rosenberg, Generation of tumor-infiltrating lymphocyte cultures for use in adoptive transfer therapy for melanoma patients. *J Immunother* 26, 332-342 (2003).
28. L. W. Collison, D. A. Vignali, In vitro Treg suppression assays. *Methods Mol Biol* 707, 21-37 (2011).
29. W. Ai, H. Li, N. Song, L. Li, H. Chen, Optimal method to stimulate cytokine production and its use in immunotoxicity assessment. *Int J Environ Res Public Health* 10, 3834-3842 (2013).
30. S. J. Szabo *et al.*, A novel transcription factor, T-bet, directs Th1 lineage commitment. *Cell* 100, 655-669 (2000).
31. X. O. Yang *et al.*, T helper 17 lineage differentiation is programmed by orphan nuclear receptors ROR alpha and ROR gamma. *Immunity* 28, 29-39 (2008).
32. J. Zhu, H. Yamane, J. Cote-Sierra, L. Guo, W. E. Paul, GATA-3 promotes Th2 responses through three different mechanisms: induction of Th2 cytokine production, selective growth of Th2 cells and inhibition of Th1 cell-specific factors. *Cell Res* 16, 3-10 (2006).
33. W. Chen *et al.*, Conversion of peripheral CD4+CD25- naive T cells to CD4+CD25+ regulatory T cells by TGF-beta induction of transcription factor Foxp3. *J Exp Med* 198, 1875-1886 (2003).
34. K. Matsuoka *et al.*, T-bet upregulation and subsequent interleukin 12 stimulation are essential for induction of Th1 mediated immunopathology in Crohn's disease. *Gut* 53, 1303-1308 (2004).
35. G. Hernandez-Hoyos, M. K. Anderson, C. Wang, E. V. Rothenberg, J. Alberola-Ila, GATA-3 expression is controlled by TCR signals and regulates CD4/CD8 differentiation. *Immunity* 19, 83-94 (2003).
36. L. M. Williams, A. Y. Rudensky, Maintenance of the Foxp3-dependent developmental program in mature regulatory T cells requires continued expression of Foxp3. *Nat Immunol* 8, 277-284 (2007).
37. M. De Simone *et al.*, Transcriptional Landscape of Human Tissue Lymphocytes Unveils Uniqueness of Tumor-Infiltrating T Regulatory Cells. *Immunity* 45, 1135-1147 (2016).
38. R. J. Miragaia *et al.*, Single-Cell Transcriptomics of Regulatory T Cells Reveals Trajectories of Tissue Adaptation. *Immunity* 50, 493-504 e497 (2019).

39. C. A. Chambers, M. S. Kuhns, J. G. Egen, J. P. Allison, CTLA-4-mediated inhibition in regulation of T cell responses: mechanisms and manipulation in tumor immunotherapy. *Annu Rev Immunol* 19, 565-594 (2001).
40. D. R. Jones, R. Foulger, W. J. Keune, Y. Bultsma, N. Divecha, PtdIns5P is an oxidative stress-induced second messenger that regulates PKB activation. *FASEB J* 27, 1644-1656 (2013).
41. H. Chi, Regulation and function of mTOR signalling in T cell fate decisions. *Nat Rev Immunol* 12, 325-338 (2012).
42. C. Liu, N. M. Chapman, P. W. Karmaus, H. Zeng, H. Chi, mTOR and metabolic regulation of conventional and regulatory T cells. *J Leukoc Biol* 97, 837-847 (2015).
43. R. Abu-Eid *et al.*, Selective inhibition of regulatory T cells by targeting the PI3K-Akt pathway. *Cancer Immunol Res* 2, 1080-1089 (2014).
44. M. Bostick *et al.*, UHRF1 plays a role in maintaining DNA methylation in mammalian cells. *Science* 317, 1760-1764 (2007).
45. Y. Obata *et al.*, The epigenetic regulator Uhrf1 facilitates the proliferation and maturation of colonic regulatory T cells. *Nat Immunol* 15, 571-579 (2014).
46. K. A. Helmin *et al.*, Maintenance DNA methylation is essential for regulatory T cell development and stability of suppressive function. *J Clin Invest* 130, 6571-6587 (2020).
47. K. A. Gelato *et al.*, Accessibility of different histone H3-binding domains of UHRF1 is allosterically regulated by phosphatidylinositol 5-phosphate. *Mol Cell* 54, 905-919 (2014).
48. J. H. Clarke *et al.*, The function of phosphatidylinositol 5-phosphate 4-kinase gamma (PI5P4Kgamma) explored using a specific inhibitor that targets the PI5P-binding site. *Biochem J* 466, 359-367 (2015).
49. D. G. Wang *et al.*, PIP4Ks Suppress Insulin Signaling through a Catalytic-Independent Mechanism. *Cell Rep* 27, 1991-2001 e1995 (2019).
50. V. Carricaburu *et al.*, The phosphatidylinositol (PI)-5-phosphate 4-kinase type II enzyme controls insulin signaling by regulating PI-3,4,5-trisphosphate degradation. *Proc Natl Acad Sci U S A* 100, 9867-9872 (2003).
51. D. Ramel *et al.*, PtdIns5P protects Akt from dephosphorylation through PP2A inhibition. *Biochem Biophys Res Commun* 387, 127-131 (2009).
52. Y. Stijf-Bultsma *et al.*, The basal transcription complex component TAF3 transduces changes in nuclear phosphoinositides into transcriptional output. *Mol Cell* 58, 453-467 (2015).
53. N. Ohkura, Y. Kitagawa, S. Sakaguchi, Development and maintenance of regulatory T cells. *Immunity* 38, 414-423 (2013).
54. X. Sun, Y. Cui, H. Feng, H. Liu, X. Liu, TGF-beta signaling controls Foxp3 methylation and T reg cell differentiation by modulating Uhrf1 activity. *J Exp Med* 10.1084/jem.20190550 (2019).
55. K. A. Helmin *et al.*, Maintenance DNA methylation is essential for regulatory T cell development and stability of suppressive function. *bioRxiv* 10.1101/2020.02.03.926949, 2020.2002.2003.926949 (2020).
56. L. Wang *et al.*, Foxp3+ T-regulatory cells require DNA methyltransferase 1 expression to prevent development of lethal autoimmunity. *Blood* 121, 3631-3639 (2013).
57. M. Alhosin *et al.*, Signalling pathways in UHRF1-dependent regulation of tumor suppressor genes in cancer. *J Exp Clin Cancer Res* 35, 174 (2016).
58. J. G. Jude *et al.*, A targeted knockdown screen of genes coding for phosphoinositide modulators identifies PIP4K2A as required for acute myeloid leukemia cell proliferation and survival. *Oncogene* 34, 1253-1262 (2015).
59. M. Kitagawa *et al.*, Dual blockade of the lipid kinase PIP4Ks and mitotic pathways leads to cancer-selective lethality. *Nat Commun* 8, 2200 (2017).
60. T. D. Manz *et al.*, Discovery and Structure-Activity Relationship Study of (Z)-5-Methylenethiazolidin-4-one Derivatives as Potent and Selective Pan-phosphatidylinositol 5-Phosphate 4-Kinase Inhibitors. *J Med Chem* 10.1021/acs.jmedchem.0c00227 (2020).

Figure legends.

Figure 1. Silencing of PIP4K2B or PIP4K2C impairs FOXP3 expression in TCR stimulated Naive T cells and Treg differentiation. A) Graphical representation of the isolation/stimulation and transduction of CD4+ Naive T cells. B) PIP4Ks were silenced using different sh_RNAs targeting PIP4Ks isoforms (sh_2A, sh_2B, sh_2C) as indicated and mRNA expression was analysed using qRT-PCR and compared to control (sh_Ctrl). C) qRT_PCR analysis of expression of transcription factors for Th1 (Tbx21/T-bet), Th2 (GATA3) and Treg (FOXP3) in cells depleted of PIP4Ks (n=3 for sh2A#1-2, n >5 for sh_Ctrl, sh_2B#1-2 and sh_2C#1-2). D) FACS analyses of T-Bet, GATA3 and FOXP3 protein levels after PIP4K2B and PIP4K2C silencing (representative of n=5). E) PIP4Ks were silenced in Naïve T cells differentiated into Tregs and FOXP3 gene expression was assessed by qRT-PCR (n=4). F) Protein levels of FOXP3 in differentiated Tregs were analysed by FACS. G) Mean Fluorescence Intensity (MFI) quantitation of FOXP3 staining from independent experiments shown in F) (n=9 for sh_Ctrl and n=7 for sh_2B#1-2 and sh_2C#1-2). Bar charts represent means with SD. Statistical analyses were performed using unpaired t-test, * pVal < 0,05, ** pVal < 0,01, *** pVal < 0,001. Number of replicates (n) refers to individual healthy donors.

Figure 2. PIP4K2B and PIP4K2C regulates FOXP3 expression and suppressive capacity of human Treg cells. A) Graphical representation of isolation/stimulation and lentiviral transduction of Treg cells. B) FACS analysis of FOXP3 expression in Tregs compared to Tconv cells. C) Western Blotting analysis of PIP4K2B and PIP4K2C silencing in Treg cells using indicated sh_RNAs. D) FACS analyses of FOXP3 levels in Treg cells after silencing of PIP4K2B or PIP4K2C obtained as in C), and Treg where PIP4Ks expression was rescued in the cells (PIP4K2B : sh_2B/OV_2B and PIP4K2C : sh_2C/OV_2C). E) Mean Fluorescence Intensity (MFI) quantitation of FOXP3 staining of experiments in D) (n=≥6 for sh_2B and sh_2C, n=4 for rescue experiments (sh_2B/OV_2B and sh_2C/OV_2C and sh_Ctrl/pCDH_E). F) Suppression assay showing Tconv proliferation upon co-culture with Treg cells depleted of PIP4K2B (sh_2B#1/#2) or PIP4K2C (sh_2C#1/#2) at different Treg/Tconv ratios. Empty pLKO_1 vector was used as a non-targeting control (sh_Ctrl), and Tconv not stimulated (NS) or TCR stimulated (ST) were employed as negative and positive controls to gate proliferating cells. G) Suppression index (diminished proliferation of Tconv cells) quantitation of experiments represented in F) (n=6 for sh_Ctrl, n=5 for sh_2B#1 and sh_2C#1, n=4 for sh_2B#2 and sh_2C#2). Bar charts represent means with SD. Statistical analyses were performed using unpaired t-test, * pVal < 0,05, ** pVal < 0,01, *** pVal < 0,001. Number of replicates (n) refers to individual healthy donors.

Figure 3. PIP4K2B and PIP4K2C regulate Treg cells transcriptomic profile. A) Volcano plots (log fold change against -log of the adjusted p-value) of expressed genes in Tregs after depletion of PIP4K2B (left panel) or PIP4K2C (right panel). The numbers and dots in blue and red refer to genes that are significantly downregulated or upregulated respectively (p<0.05 and absolute log2fold change>0.6). B) Same as A) except PIP4K depletions were in Tconv cells. In both A) and B) the x and y axis have the same minimum

and maximum to illustrate the difference in effects of PIP4K depletions in Tregs compared to Tconv. C) Scatter plots to show the changes in the expression of genes from the Treg_shPIP4K-DEG geneset after depletion of PIP4K in either Tregs or Tconvs as indicated. Left panel: depletion of PIP4K2B (log(sh_2B/sh_Ctrl) plotted on the x axis and PIP4K2C depletion (log(sh_2C/sh_Ctrl) on the y axis. Middle panel: depletion of PIP4K2B in Tregs against depletion of PIP4K2B in Tconv cells. Right panel: depletion of PIP4K2C in Tregs against depletion of PIP4K2C in Tconv cells. The data depict the average of three RNA-seq data sets for each knockdown in Treg and two in Tconvs. D) The Treg_shPIP4K-DEG gene set was used for PCA analysis. E) Left panel: the Treg_shPIP4K-DEG (*p*-adjusted<0.05) was used to generate a heatmap with scaled rows and three hierarchical clusters. Right panel: gene sets from each cluster were extracted and the average expression of genes within each cluster in Tregs and Tconv before and after depletion of PIP4Ks were quantitated. F) Genes from cluster 3 (E) were used to interrogate their expression in an unrelated dataset comprising Tconv and Tregs before (Tconv_NS, Treg_NS) and after CD3/CD28 activation (Tconv_ST, Treg_ST) isolated from four separate donors. The heatmap shows the average expression of each gene within cluster 3, while the graph depicts the average expression of all genes from cluster 3. The data illustrate that cluster 3 genes are upregulated upon T-cell activation. G) GO enrichment analysis showing that cluster 3 genes are highly enriched for genes related to cell cycle, mitosis and chromosome segregation. Box plots follow standard Tukey representation. Statistics are derived using Krushkal Wallis hypothesis testing with post hoc paired testing using BH probability adjustments.

Figure 4. PIP4K2B and PIP4K2C silencing specifically inhibits TCR dependent signalling and activation of Tregs compared to Tconv cells. A) PIP4K2B and PIP4K2C were silenced in Tregs (top panel) and in Tconv (bottom panel) and stimulated or not (CD3/CD28 stimulation) for 1 hour. Activation of PI3K, MAPK and mTORC1 signalling was assessed by western blotting using the indicated antibodies. B) Quantitation of experiments shown in A) in Tregs (top panel) and in Tconv (bottom panel) upon PIP4Ks depletion and presented after normalization to sh_Ctrl NS and Histone 3A (n=4). C) Proliferation analysis by FACS (Cell Trace dye dilution) of Tregs (top panel) and Tconv (bottom panel) upon PIP4K silencing as indicated. D) Quantitative data for experiments in G) are presented (n=5). E) Cell apoptosis was analysed by FACS (Annexin-V staining) in Tregs (top panel) and Tconv (bottom panel) upon PIP4Ks silencing (see C). F) Quantitative data are presented for the experiments in E) (n=5). G and H) PI3K inhibition impacts on FOXP3 levels. Expanded Treg cells (top panel) and *in vitro* differentiated Treg cells (bottom panel) were treated with Rapamycin (100nm) or CAL-101 (10μM) and levels of FOXP3 were analysed by FACS. DMSO was used as vehicle control (n=3). Bar charts represent means with SD. Statistical analyses were performed using unpaired t-test, * pVal < 0,05, ** pVal < 0,01, *** pVal < 0,001. Number of replicates (n) refers to individual healthy donors.

Figure 5. PIP4K depletion decreases UHRF1 levels in Tregs altering immunosuppressive capacity and cell viability. A) Treg cells were TCR stimulated for the times indicated and the expression of UHRF1 and FOXP3 was measured by qRT-PCR. B) Expression levels of UHRF1 in Tregs (left panel) and Tconv (right panel) cells upon PIP4K silencing as indicated was analysed using qRT-PCR (n=3). Empty pLKO_1 vector was used as control (sh_Ctrl). C) Western Blotting analysis of the expression levels of UHRF1 in Treg cells depleted of PIP4K or UHRF1 as indicated compared to control cells (sh_Ctrl). D) Tregs were treated with p110δ inhibitor (CAL-101, 10μM) for 24 or 48h and the expression of UHRF1 (left panel) or FOXP3 (right panel) was assessed using qRT-PCR (n=3). DMSO was used as vehicle control. E) UHRF1 was silenced in Tregs (sh_UHRF1) and expression of UHRF1 (left panel) and of FOXP3 (right panel) were measured using qRT-PCR (n=3). F/G/H/I) UHRF1 was silenced and protein levels of FOXP3 (F) or CTLA4 (H) were measured by FACS. MFI values of FOXP3 (G) and CTLA4 (I) expression were quantitated after UHRF1 depletion (n=3). J) UHRF1 was silenced in Tregs and their immunosuppressive activity towards T conv cells was assessed (representative of n=3). K) UHRF1 was silenced in Tregs and apoptosis was assessed by Annexin-V staining (representative of n=3). Bar charts represent means with SD. Statistical analyses were performed using unpaired t-test, * pVal < 0,05, ** pVal < 0,01, *** pVal < 0,001. Number of replicates (n) refers to individual healthy donors.

Figure 6. Pharmacological Inhibition of PIP4K2C with NIH-12848 phenocopies PIP4K2C silencing in Treg cells. A) Treg cells were treated with DMSO or NIH-12848 (20uM) for 48 hours, then TCR stimulated (+) or maintained as controls (-). Lysates were probed with the indicated antibodies by western blotting (representative of n=3). Tregs were treated with DMSO or NIH-12848 for 48h at the concentrations indicated and cell proliferation (B), apoptosis (C) or FOXP3 levels (D) were measured by FACS (representative of n=3). E) Inhibition of PIP4K2C affects Treg cells capacity to suppress Tconv proliferation. Quantitative data for suppressive experiments are presented (n=3). Bar charts represent means with SD. Statistical analyses were performed using unpaired t-test, * pVal < 0,05, ** pVal < 0,01, *** pVal < 0,001. Number of replicates (n) refers to individual healthy donors.

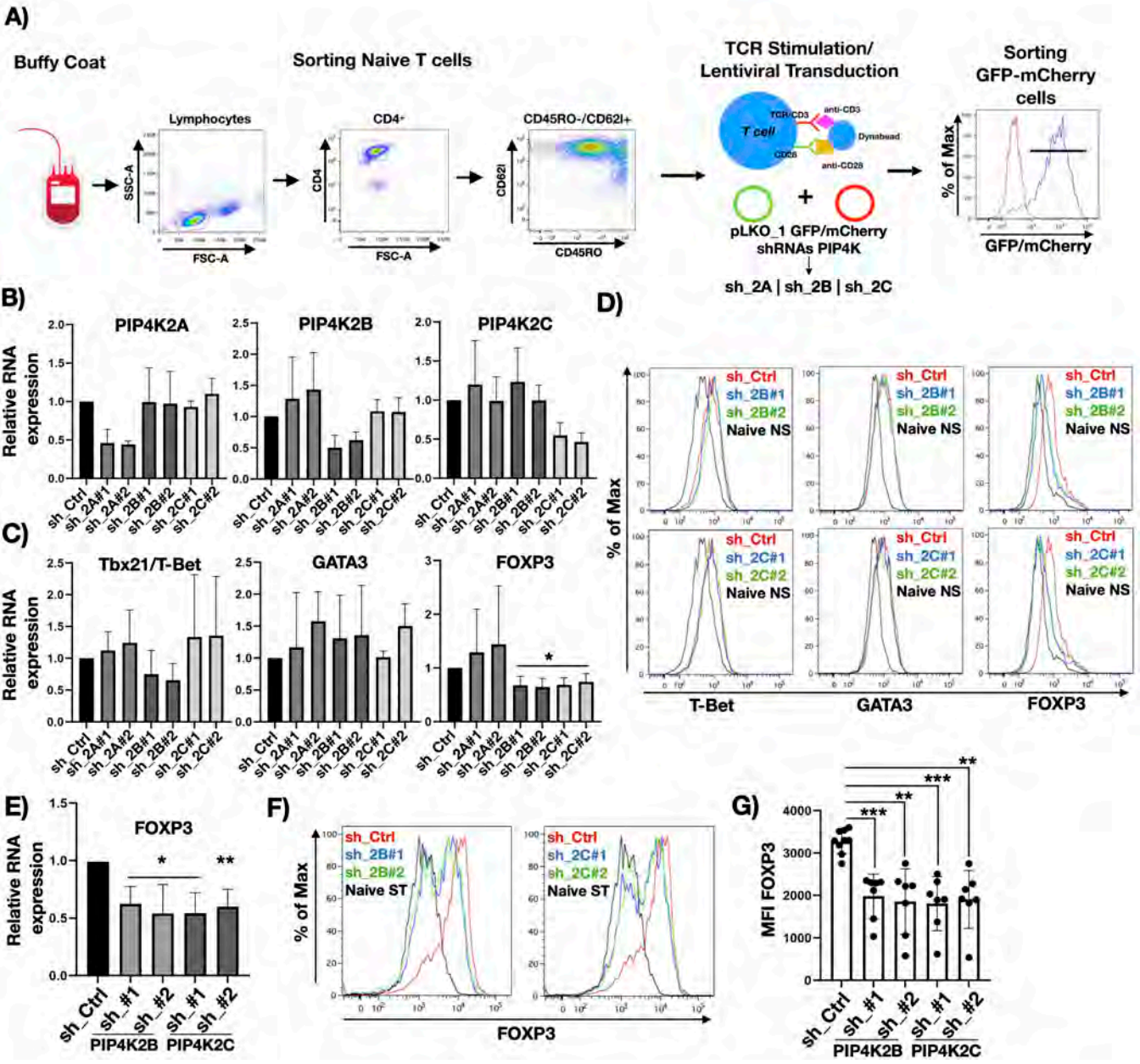
A)
Buffy Coat
Sorting Naive T cells
Lymphocytes
SSC-A
FSC-A
CD4+
CD4
FSC-A
CD45RO-/CD62l+
CD62l
CD45RO
TCR Stimulation/
Lentiviral Transduction
T cell
TCR/CD3
anti-CD3
Dynabead
CD28
anti-CD28
pLKO_1 GFP/mCherry
shRNAs PIP4K
sh_2A | sh_2B | sh_2C
Sorting
GFP-mCherry
cells
% of Max
GFP/mCherry
B)
PIP4K2A
PIP4K2B
PIP4K2C
Relative RNA expression
sh_Ctrl
sh_2A#1
sh_2A#2
sh_2B#1
sh_2B#2
sh_2C#1
sh_2C#2
C)
Tbx21/T-Bet
GATA3
FOXP3
*
D)
% of Max
sh_Ctrl
sh_2B#1
sh_2B#2
sh_2C#1
sh_2C#2
Naive NS
T-Bet
GATA3
FOXP3
E)
FOXP3
Relative RNA expression
*
**
sh_Ctrl
sh_#1
sh_#2
sh_#1
sh_#2
PIP4K2B
PIP4K2C
F)
% of Max
sh_Ctrl
sh_2B#1
sh_2B#2
sh_2C#1
sh_2C#2
Naive ST
FOXP3
G)
MFI FOXP3
***
**
***
**
sh_Ctrl
sh_#1
sh_#2
sh_#1
sh_#2
PIP4K2B
PIP4K2C

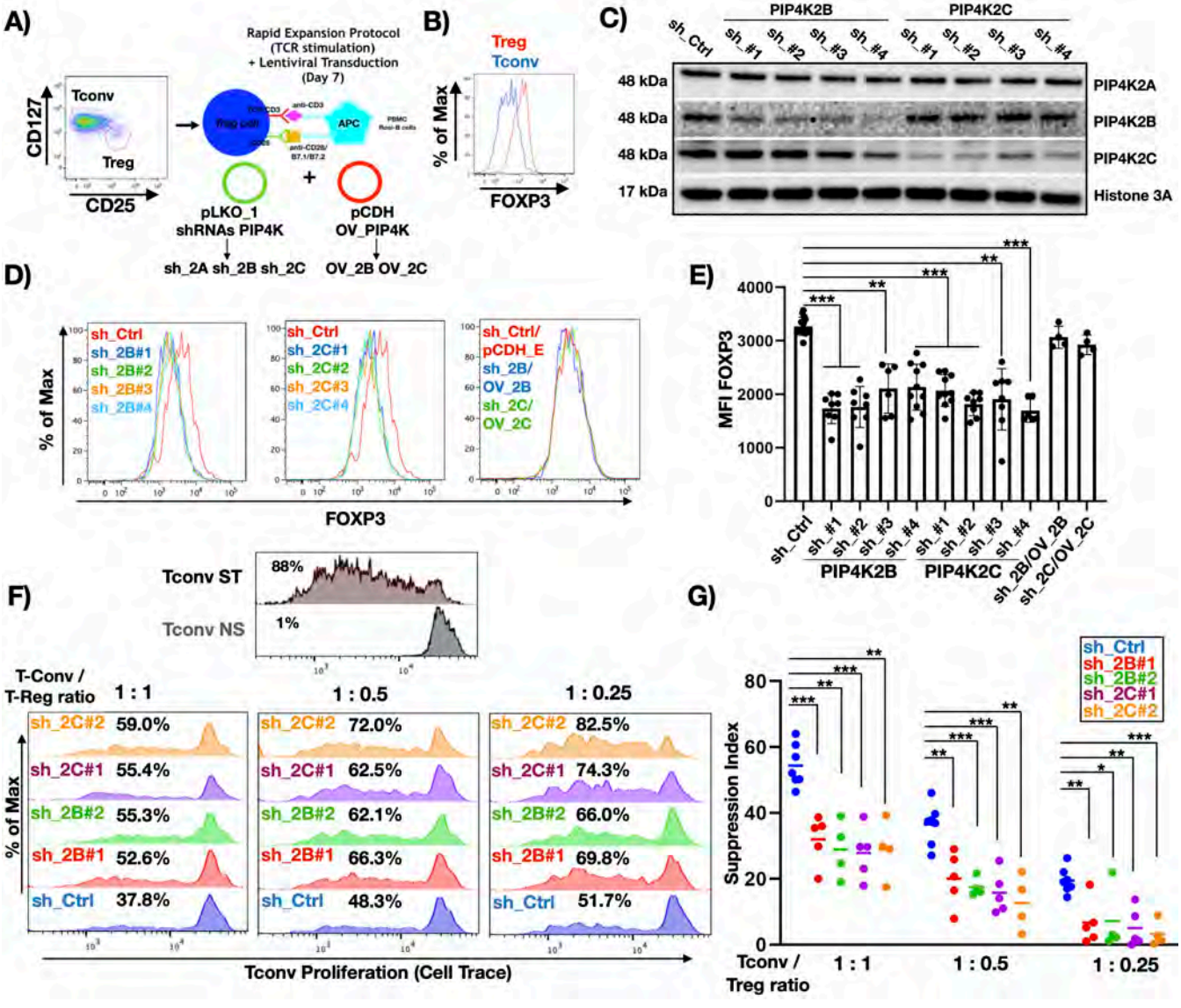
A)
Rapid Expansion Protocol
(TCR stimulation)
+ Lentiviral Transduction
(Day 7)
Tconv
Treg
CD127
CD25
anti-CD3
APC
PBMC
Resp-B cells
anti-CD28/
B7.1/B7.2
pLKO_1
shRNAs PIP4K
sh_2A sh_2B sh_2C
pCDH
OV_PIP4K
OV_2B OV_2C
B)
Treg
Tconv
% of Max
FOXP3
C)
PIP4K2B
PIP4K2C
sh_Ctrl
sh_#1
sh_#2
sh_#3
sh_#4
48 kDa
48 kDa
48 kDa
17 kDa
PIP4K2A
PIP4K2B
PIP4K2C
Histone 3A
D)
sh_Ctrl
sh_2B#1
sh_2B#2
sh_2B#3
sh_2B#4
sh_2C#1
sh_2C#2
sh_2C#3
sh_2C#4
sh_Ctrl/
pCDH_E
sh_2B/
OV_2B
sh_2C/
OV_2C
% of Max
FOXP3
E)
MFI FOXP3
4000
3000
2000
1000
0
sh_Ctrl
sh_#1
sh_#2
sh_#3
sh_#4
PIP4K2B
PIP4K2C
sh_2B/OV_2B
sh_2C/OV_2C
F)
Tconv ST
88%
Tconv NS
1%
T-Conv /
T-Reg ratio
1 : 1
1 : 0.5
1 : 0.25
sh_2C#2 59.0%
sh_2C#1 55.4%
sh_2B#2 55.3%
sh_2B#1 52.6%
sh_Ctrl 37.8%
sh_2C#2 72.0%
sh_2C#1 62.5%
sh_2B#2 62.1%
sh_2B#1 66.3%
sh_Ctrl 48.3%
sh_2C#2 82.5%
sh_2C#1 74.3%
sh_2B#2 66.0%
sh_2B#1 69.8%
sh_Ctrl 51.7%
% of Max
Tconv Proliferation (Cell Trace)
G)
sh_Ctrl
sh_2B#1
sh_2B#2
sh_2C#1
sh_2C#2
Suppression Index
80
60
40
20
0
Tconv /
Treg ratio
1 : 1
1 : 0.5
1 : 0.25

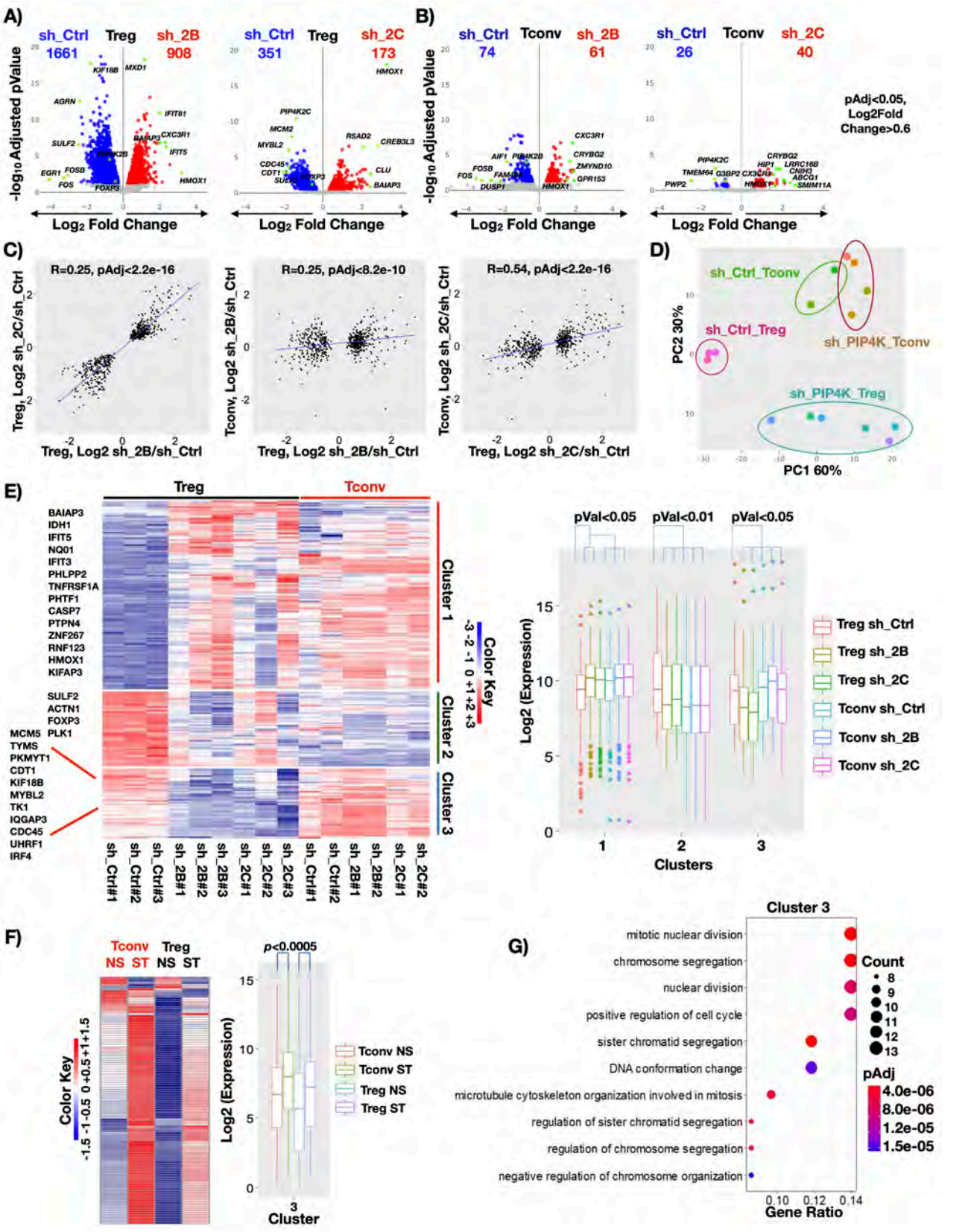
A)
sh_Ctrl
Treg
sh_2B
1661
908
sh_Ctrl
Treg
sh_2C
351
173
-log10 Adjusted pValue
Log2 Fold Change
KIF18B
MXD1
AGRN
IFIT81
SULF2
BAIAP3
CXC3R1
PHPK2B
IFIT5
EGR1
FOSB
FOS
FOXP3
HMOX1
PIP4K2C
MCM2
MYBL2
RSAD2
CREB3L3
CDC45
CDT1
SULF2
FOXP3
CLU
BAIAP3
HMOX1
B)
sh_Ctrl
Tconv
sh_2B
74
61
sh_Ctrl
Tconv
sh_2C
26
40
pAdj<0.05,
Log2Fold
Change>0.6
CXC3R1
AIF1
PIP4K2B
CRYBG2
FOSB
ZMYND10
FOS
FAM49A
GPR153
DUSP1
HMOX1
PIP4K2C
CRYBG2
HIP1
LRRC16B
TMEM64
G3BP2
CX3CR1
CNIH3
ABCG1
HMOX1
PWP2
SMIM11A
C)
R=0.25, pAdj<2.2e-16
R=0.25, pAdj<8.2e-10
R=0.54, pAdj<2.2e-16
Treg, Log2 sh_2C/sh_Ctrl
Tconv, Log2 sh_2B/sh_Ctrl
Tconv, Log2 sh_2C/sh_Ctrl
Treg, Log2 sh_2B/sh_Ctrl
Treg, Log2 sh_2B/sh_Ctrl
Treg, Log2 sh_2C/sh_Ctrl
D)
sh_Ctrl_Tconv
sh_Ctrl_Treg
sh_PIP4K_Tconv
sh_PIP4K_Treg
PC2 30%
PC1 60%
E)
Treg
Tconv
BAIAP3
IDH1
IFIT5
NQ01
IFIT3
PHLPP2
TNFRSF1A
PHTF1
CASP7
PTPN4
ZNF267
RNF123
HMOX1
KIFAP3
SULF2
ACTN1
FOXP3
PLK1
MCM5
TYMS
PKMYT1
CDT1
KIF18B
MYBL2
TK1
IQGAP3
CDC45
UHRF1
IRF4
Cluster 1
Cluster 2
Cluster 3
Color Key
-3 -2 -1 0 +1 +2 +3
sh_Ctr#1
sh_Ctr#2
sh_Ctr#3
sh_2B#1
sh_2B#2
sh_2B#3
sh_2C#1
sh_2C#2
sh_2C#3
sh_Ctr#1
sh_Ctr#2
sh_2B#1
sh_2B#2
sh_2C#1
sh_2C#2
pVal<0.05
pVal<0.01
pVal<0.05
Log2 (Expression)
Clusters
Treg sh_Ctrl
Treg sh_2B
Treg sh_2C
Tconv sh_Ctrl
Tconv sh_2B
Tconv sh_2C
F)
Tconv
NS ST
Treg
NS ST
Color Key
-1.5 -1 -0.5 0 +0.5 +1 +1.5
p<0.0005
Log2 (Expression)
Cluster
Tconv NS
Tconv ST
Treg NS
Treg ST
G)
Cluster 3
mitotic nuclear division
chromosome segregation
nuclear division
positive regulation of cell cycle
sister chromatid segregation
DNA conformation change
microtubule cytoskeleton organization involved in mitosis
regulation of sister chromatid segregation
regulation of chromosome segregation
negative regulation of chromosome organization
Count
pAdj
Gene Ratio

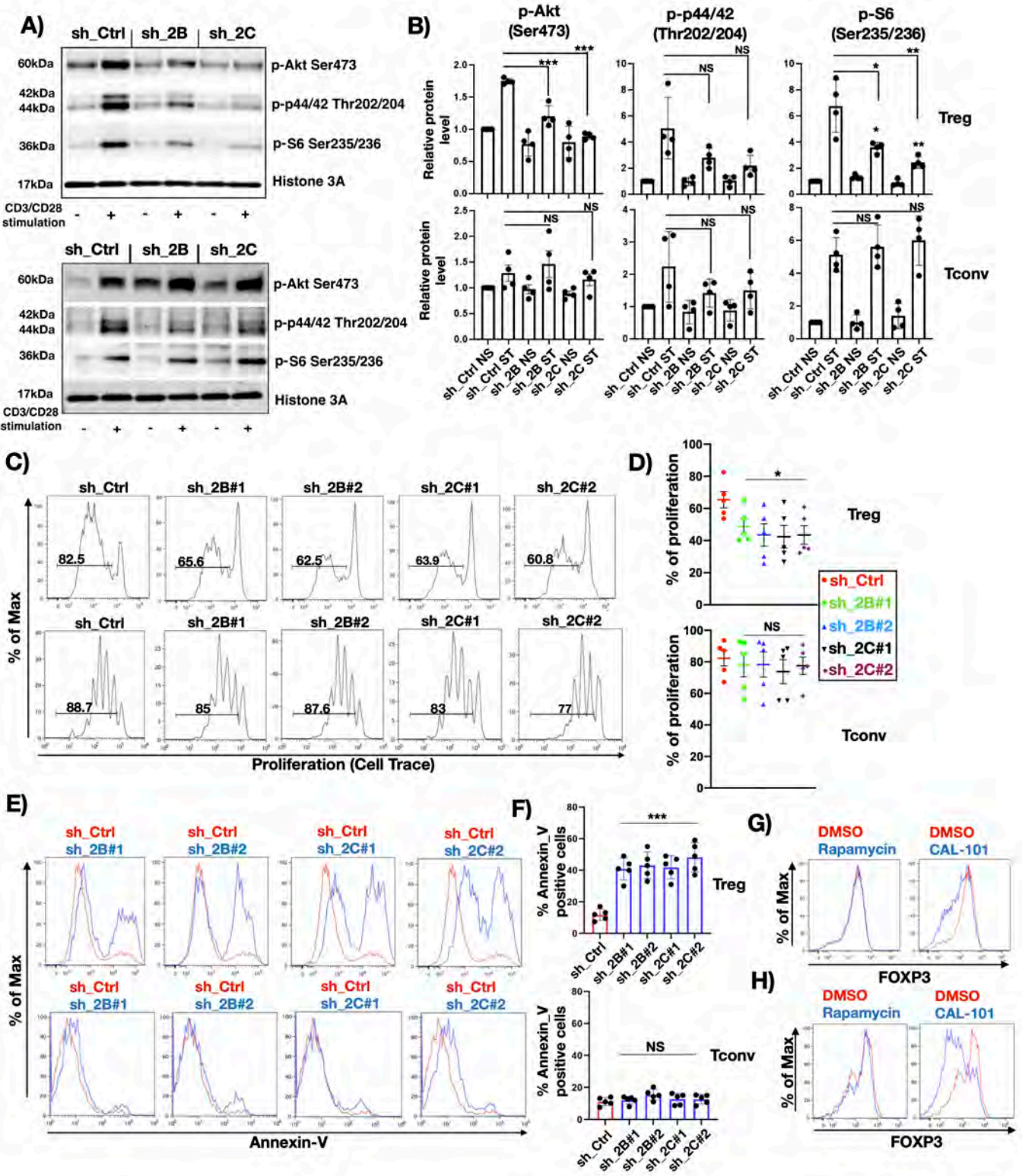
A)
sh_Ctrl
sh_2B
sh_2C
60kDa
42kDa
44kDa
36kDa
17kDa
p-Akt Ser473
p-p44/42 Thr202/204
p-S6 Ser235/236
Histone 3A
CD3/CD28 stimulation
B)
p-Akt (Ser473)
p-p44/42 (Thr202/204)
p-S6 (Ser235/236)
Relative protein level
Treg
Tconv
NS
sh_Ctrl NS
sh_Ctrl ST
sh_2B NS
sh_2B ST
sh_2C NS
sh_2C ST
C)
sh_Ctrl
sh_2B#1
sh_2B#2
sh_2C#1
sh_2C#2
82.5
65.6
62.5
63.9
60.8
88.7
85
87.6
83
77
% of Max
Proliferation (Cell Trace)
D)
% of proliferation
Treg
Tconv
E)
Annexin-V
F)
% Annexin_V positive cells
G)
DMSO
Rapamycin
CAL-101
FOXP3
H)

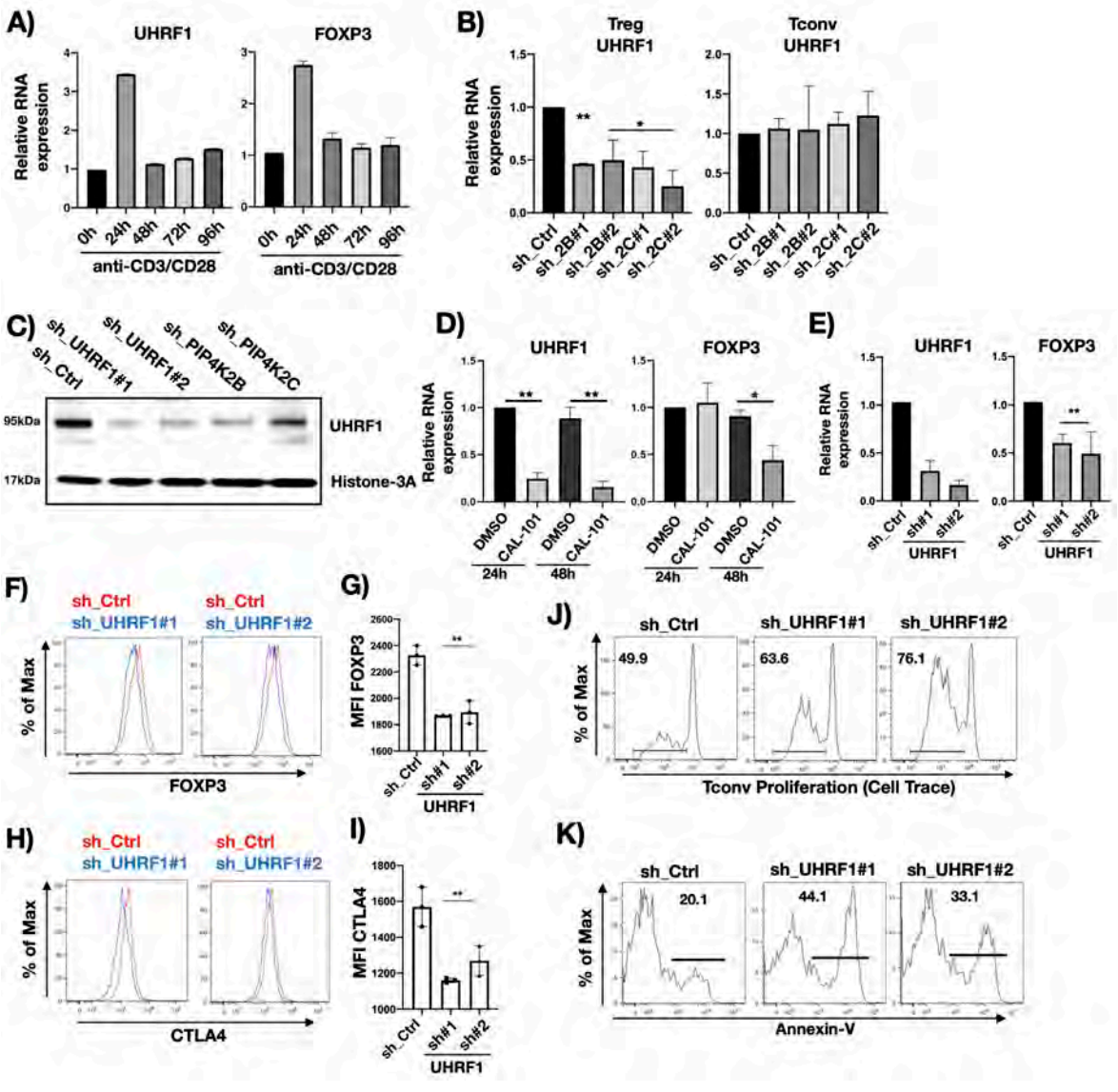
A)
UHRF1
FOXP3
Relative RNA expression
0h
24h
48h
72h
96h
anti-CD3/CD28
B)
Treg
UHRF1
Tconv
UHRF1
Relative RNA expression
**
*
sh_Ctrl
sh_2B#1
sh_2B#2
sh_2C#1
sh_2C#2
C)
sh_Ctrl
sh_UHRF1#1
sh_UHRF1#2
sh_PIP4K2B
sh_PIP4K2C
95kDa
17kDa
UHRF1
Histone-3A
D)
UHRF1
FOXP3
Relative RNA expression
DMSO
CAL-101
24h
48h
E)
UHRF1
FOXP3
Relative RNA expression
sh_Ctrl
sh#1
sh#2
UHRF1
F)
sh_Ctrl
sh_UHRF1#1
sh_Ctrl
sh_UHRF1#2
% of Max
FOXP3
G)
MFI FOXP3
sh_Ctrl
sh#1
sh#2
UHRF1
J)
sh_Ctrl
sh_UHRF1#1
sh_UHRF1#2
49.9
63.6
76.1
% of Max
Tconv Proliferation (Cell Trace)
H)
sh_Ctrl
sh_UHRF1#1
sh_Ctrl
sh_UHRF1#2
% of Max
CTLA4
I)
MFI CTLA4
sh_Ctrl
sh#1
sh#2
UHRF1
K)
sh_Ctrl
sh_UHRF1#1
sh_UHRF1#2
20.1
44.1
33.1
% of Max
Annexin-V

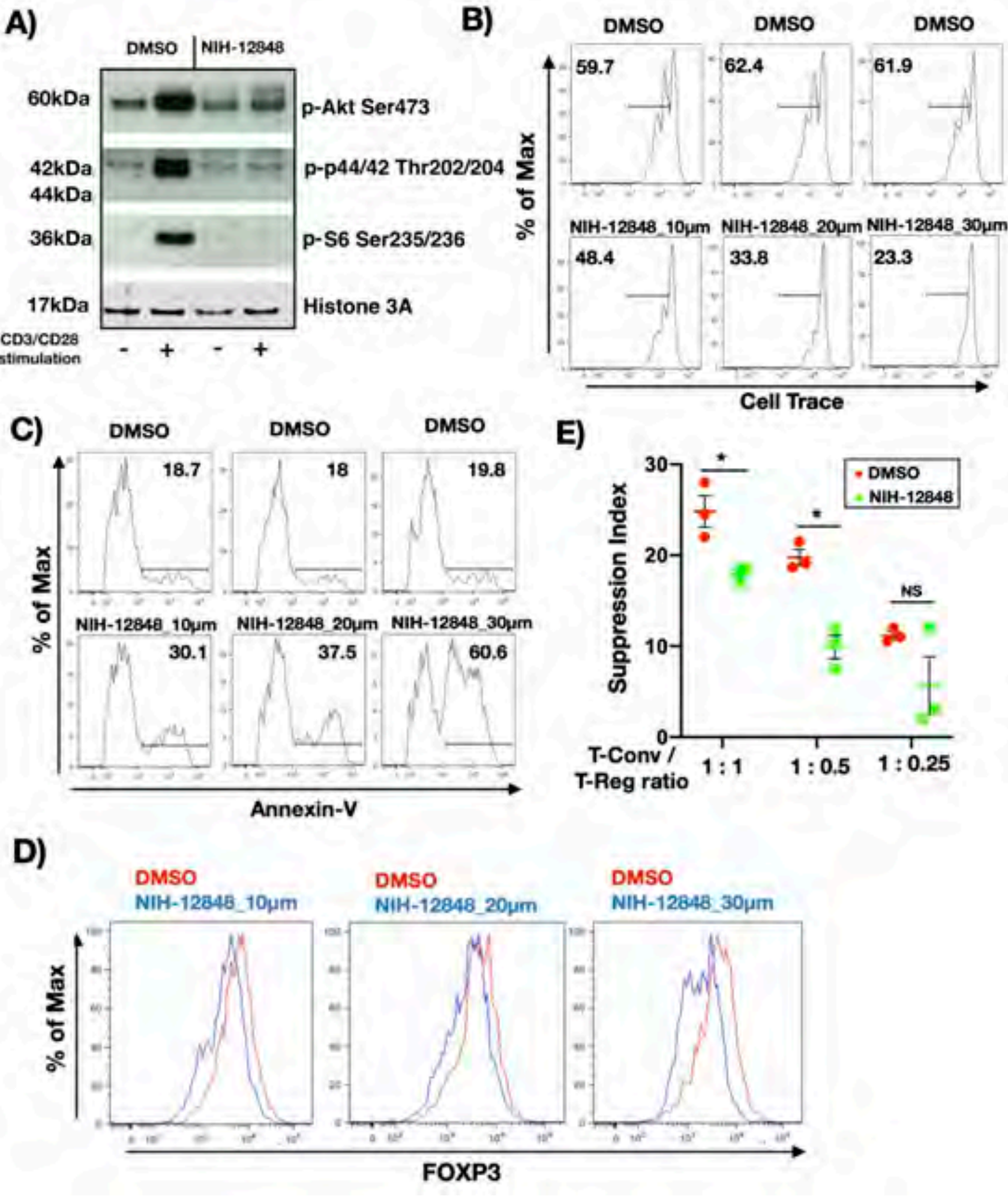
A)
DMSO
NIH-12848
60kDa
42kDa
44kDa
36kDa
17kDa
p-Akt Ser473
p-p44/42 Thr202/204
p-S6 Ser235/236
Histone 3A
CD3/CD28 stimulation
- + - +
B)
DMSO
DMSO
DMSO
59.7
62.4
61.9
NIH-12848_10µm
NIH-12848_20µm
NIH-12848_30µm
48.4
33.8
23.3
% of Max
Cell Trace
C)
DMSO
DMSO
DMSO
18.7
18
19.8
NIH-12848_10µm
NIH-12848_20µm
NIH-12848_30µm
30.1
37.5
60.6
% of Max
Annexin-V
E)
DMSO
NIH-12848
Suppression Index
30
20
10
0
*
*
NS
T-Conv / T-Reg ratio
1 : 1
1 : 0.5
1 : 0.25
D)
DMSO
NIH-12848_10µm
DMSO
NIH-12848_20µm
DMSO
NIH-12848_30µm
% of Max
FOXP3